



Sex-specific alterations in NAD⁺ metabolism in 3xTg Alzheimer's disease mouse brain assessed by quantitative targeted LC-MS

Vera van der Velpen¹ | Nadia Rosenberg² | Vanille Maillard¹ | Tony Teav¹ | Jean-Yves Chatton²  | Hector Gallart-Ayala¹ | Julijana Ivanisevic¹ 

¹Metabolomics Platform, Faculty of Biology and Medicine, University of Lausanne, Lausanne, Switzerland

²Department of Fundamental Neurosciences, Faculty of Biology and Medicine, University of Lausanne, Lausanne, Switzerland

Correspondence

Julijana Ivanisevic, Metabolomics Platform, Faculty of Biology and Medicine, University of Lausanne, Lausanne, Switzerland.
Email: Julijana.Ivanisevic@unil.ch

Present address

Vera van der Velpen, Clinical Pharmacology and Toxicology, Department of General Internal Medicine, Inselspital, Bern University Hospital, Bern, Switzerland

Funding information

Foundation Peirre-Mercier pour la science; Stiftung Synapsis - Alzheimer Forschung Schweiz AFS

This article is part of the special issue "Mass Spectrometry in Alzheimer Disease".

Abstract

Levels of nicotinamide adenine dinucleotide (NAD⁺) are known to decline with age and have been associated with impaired mitochondrial function leading to neurodegeneration, a key facet of Alzheimer's disease (AD). NAD⁺ synthesis is sustained via tryptophan-kynurenine (Trp-Kyn) pathway as de novo synthesis route, and salvage pathways dependent on the availability of nicotinic acid and nicotinamide. While being currently investigated as a multifactorial disease with a strong metabolic component, AD remains without curative treatment and important sex differences were reported in relation to disease onset and progression. The aim of this study was to reveal the potential deregulation of NAD⁺ metabolism in AD with the direct analysis of NAD⁺ precursors in the mouse brain tissue (wild type (WT) versus triple transgenic (3xTg) AD), using a sex-balanced design. To this end, we developed a quantitative liquid chromatography-tandem mass spectrometry (LC-MS/MS) method, which allowed for the measurement of the full spectrum of NAD⁺ precursors and intermediates in all three pathways. In brain tissue of mice with developed AD symptoms, a decrease in kynurenine (Kyn) versus increase in kynurenic acid (KA) levels were observed in both sexes with a significantly higher increment of KA in males. These alterations in Trp-Kyn pathway might be a consequence of neuroinflammation and a compensatory production of neuroprotective kynurenic acid. In the NAD⁺ salvage pathway, significantly lower levels of nicotinamide mononucleotide (NMN) were measured in the AD brain of males and females. Depletion of NMN implies the deregulation of salvage pathway critical for maintaining optimal NAD⁺ levels and mitochondrial and neuronal function.

Abbreviations: 3HAA, 3-hydroxyanthranilic acid; 3HK, 3-hydroxy-kynurenine; 3xTg, triple transgenic; AA, anthranilic acid; AD, Alzheimer's Disease; ANOVA, analysis of variance; CD38, cyclic ADP ribose hydrolase; CE, collision energy; CNS, central nervous system; CSF, cerebrospinal fluid; CV, coefficient of variation; ESI, electrospray ionization; FDR, false discovery rate; HILIC, hydrophilic interaction chromatography; IS, internal standard; KA, kynurenic acid; KYN, kynurenine; LC-MS, liquid chromatography-mass spectrometry; LC-MS/MS, liquid chromatography-tandem mass spectrometry; LOQ, limit of quantification; MCI, mild cognitive impairment; MRM, multiple reaction monitoring; MS, mass spectrometry; NA, nicotinic acid; NaAD, nicotinic acid adenine dinucleotide; NAD⁺, nicotinamide adenine dinucleotide; NADH, reduced nicotinamide adenine dinucleotide; NaMN, nicotinic acid mononucleotide; NaR, nicotinic acid riboside; NMN, nicotinamide mononucleotide; NR, nicotinamide riboside; PA, picolinic acid; PARP, poly ADP ribose polymerase; QA, quinolinic acid; QQQ, triple quadrupole; RPLC, reversed phase liquid chromatography; RRID, Research Resource Identifier (see scicrunch.org); RT, retention time; SIRT, sirtuins, a family of histone deacetylases; TCA cycle, tricarboxylic acid cycle; TRP, tryptophan; UHPLC, ultra-high performance liquid chromatography; WT, wild type; XA, xanthurenic acid.

Hector Gallart-Ayala and Julijana Ivanisevic, equally contributing senior authors.

This is an open access article under the terms of the Creative Commons Attribution-NonCommercial License, which permits use, distribution and reproduction in any medium, provided the original work is properly cited and is not used for commercial purposes.

© 2021 The Authors. *Journal of Neurochemistry* published by John Wiley & Sons Ltd on behalf of International Society for Neurochemistry.



KEYWORDS

3xTg AD mouse model, Alzheimer's disease, brain, LC-MS, NAD⁺ metabolism, targeted metabolomics

1 | INTRODUCTION

In recent years, nicotinamide adenine dinucleotide (NAD⁺) has been recognized as a major player in biological processes (i.e., DNA repair, protein activity, signal transduction, gene silencing, aging, and cell death) essential for the maintenance of organismal health, beyond its role as the coenzyme in energy generating pathways, such as TCA cycle and oxidative phosphorylation (Canto et al., 2015; Houtkooper et al., 2010; Katsyuba & Auwerx, 2017). Three interconnected pathways are known to sustain NAD⁺ production: de novo synthesis (starting with tryptophan-kynurenine pathway), the nicotinamide-based salvage pathway (using nicotinamide – NAM and/or nicotinamide riboside – NR as substrates), and the nicotinic acid-based salvage or Preiss-Handler pathway (with nicotinic acid – NA and nicotinic acid riboside – NaR as main substrates).

Numerous studies have reported the decline in NAD⁺ levels with age, in blood plasma in humans (Clement et al., 2019; Imai & Guarente, 2014; Massudi et al., 2012), and across different tissues such as liver, skeletal muscle and kidney in model organisms (Yaku et al., 2018a, 2018b). Reduced NAD⁺ levels were also found in the aging human brain (Zhu et al., 2015) and have been linked to neurodegenerative diseases, such as late-onset Alzheimer's disease (AD), for which age is the main risk factor (Lautrup et al., 2019). Alzheimer's disease is a multifactorial disease with complex etiology and strong metabolic character for which a curative treatment is still lacking (Scheltens et al., 2016). Metabolic alterations are manifested at the central nervous system (CNS) as well as the systemic level (van der Velpen et al., 2019), and therefore it is important to further monitor and unravel affected biochemical pathways associated with AD phenotype. This is particularly relevant when taking into account sex differences, an often-overlooked aspect in AD studies. For instance, considerable sex differences in AD prevalence were reported, that is, two-thirds of the AD patients are women (2020), and disease progression, for example, the rate of cognitive decline in women appears to be higher than in men (Ferretti et al., 2018). However, no consensus to date exists on the underlying demographic and/or biological causes for these sex differences that are still not systematically studied in AD (Mielke, 2018). A few recent studies have suggested that sex differences also exist at the metabolite level (Arnold et al., 2020; Darst et al., 2019). In our previous work, we have also observed the female-specific and AD pathology-associated changes in the cerebrospinal fluid (CSF) levels of kynurenine metabolites.

NAD⁺ synthesis is targeted in multiple research studies with the aim of boosting the NAD⁺ production (Katsyuba et al., 2018; Rajman et al., 2018; Shi et al., 2017), considered as essential for the mitochondrial function and to improve the health outcome of

age-associated metabolic diseases, such as AD (Hikosaka et al., 2021; Mitchell et al., 2018; Mouchiroud et al., 2013). In this context, the accurate and highly specific measurement of multiple NAD⁺ precursors (tryptophan, NA, NaR, NAM, and NR) coming from diet and their intermediates (NaMN, NaAD, and NMN) in synthesis pathways is necessary to elucidate important mechanistic insights into potential routes of intervention.

The active small molecule complement of biofluids and tissues can be measured with high specificity, accuracy, and precision through the widely accepted methodological approach of targeted metabolite analysis using liquid chromatography coupled to tandem mass spectrometry (LC-MS/MS) (Gallart-Ayala et al., 2020; Lu et al., 2008; Roberts et al., 2012). For NAD⁺ metabolism, the robustness of LC-MS methodology was demonstrated with the quantification of intermediates in tryptophan-kynurenine pathway (route for de novo NAD⁺ synthesis), applied to large-scale population studies (Sadok et al., 2019; Whiley et al., 2019; Yu et al., 2018). However, the robust method for the quantification of NAD⁺ and its direct precursors from the salvage pathways (including Preiss-Handler pathway) is still lacking (Rubio et al., 2020). Particularly challenging is to achieve the sufficient chromatographic resolution required for the accurate quantification of metabolite pairs with 1 Da difference in these pathways, such as NAD/NaAD, NA/Nicotinamide, NR/NaR, and NMN/NaMN. Previously developed methods either do not cover all these metabolites (and omit to highlight the potential bias introduced by the presence of respective "pair" metabolites) or present long runs (Bustamante et al., 2017; Giroud-Gerbetant et al., 2019; Martino Carpi et al., 2018; Ratajczak et al., 2016).

Here, we developed a quantitative LC-MS/MS method to (1) comprehensively assess NAD⁺ metabolism by covering the entire panel of intermediates from the three different pathways (i.e., the tryptophan-kynurenine pathway leading to NAD⁺ de novo synthesis, the Preiss-Handler pathway, and the nicotinamide-based salvage pathway) and (2) investigate the potential alterations in NAD⁺ metabolism associated with AD, while considering sex differences. To this end, we used the triple transgenic AD (3xTg AD) mouse model that recapitulates key features of AD in humans. Because of the gene mutations of human presenilin-1 M146V (PS1M146V), human amyloid precursor protein Swedish mutation (APP^{Swe}), and the P301L mutation of human tau (tauP301L), this model shows AD-related accumulation of A β plaques, intraneuronal Tau Tangles, and cognitive impairment (Oddo et al., 2003). The exploration of potential deregulation in NAD⁺ balance in brain tissue of 8-month-old 3xTg AD mice exhibiting cognitive impairment, plaques, and gliosis was useful to determine the metabolic alterations in the disease stage preceding the accumulation of Tau tangles and neuronal death, equivalent to the stage for which the unambiguous clinical symptoms in humans remain scarce.

2 | MATERIALS AND METHODS

2.1 | Reagents and chemicals

LC-MS grade water (cat. no. 232141) and organic solvent (methanol, cat. no. 136841) and formic acid (cat. no. 069141) were purchased from Biosolve Chimie (Dieuze, France), while ammonium formate was obtained from Merck (cat. no. 70221, Darmstadt, Germany). The analytical standards and isotopically labeled standards (Table S1, incl. cat. no's) were obtained from Merck, Cayman Chemical Company, Carbosynth (Compton, UK), Toronto Research Chemicals (North York, Ontario, Canada), and Cambridge Isotopes Laboratories.

2.2 | Standard solutions and calibration curves

Individual stock solutions of each metabolite were prepared in water at concentrations ranging from 0.1 to 5 mM. These solutions were then mixed and completed with water to achieve the final metabolite concentration ranging from 5 μ M to 1,000 μ M depending on the metabolite and according to the concentration levels reported in the literature for human plasma and brain tissue (Wishart et al., 2018). Starting from this final (i.e., highest concentration) standard mixture, the calibrators were prepared by serial dilutions with water. These calibrators were used to determine the instrumental limits of quantification (LOQs) and the calibration range and coefficients of determination are provided in Table S2. In addition, internal standard (IS) mixture was prepared using 11 deuterium, ^{13}C -, and ^{15}N -labeled compounds. The IS mixture was prepared in water with IS concentrations ranging from 0.2 μ M to 20 μ M, depending on the metabolite.

2.3 | Sample and calibration curve preparation

For absolute quantification of the intermediates implicated in NAD⁺ de novo synthesis and salvage pathway, samples were prepared by spiking 100 μ l of tissue extract with 25 μ l of internal standard solution and then sample extracts were evaporated to dryness using a centrivap centrifugal vacuum concentrator (Labconco). Dry extracts were subsequently reconstituted with 75 μ l of water and injected into the LC-MS/MS system.

2.4 | LC-MS/MS method optimization

An Agilent 1,290 Infinite (Agilent Technologies) ultra-high performance liquid chromatography (UHPLC) system coupled to Agilent 6,495 triple quadrupole mass spectrometer equipped with an Agilent Jet Stream ESI source was used for the quantification of the intermediates implicated in NAD⁺ de novo synthesis, salvage, and Preiss-Handler pathway. To optimize the chromatographic conditions, several hydrophilic interaction liquid chromatography (HILIC, including ZIC-pHILIC, Phenomenex Luna-NH2, and BEH Amide)

and reversed phase (RPLC) columns (HSS T3, BEH C18, and Scherzo SM-C18) were evaluated, in acidic (pH = 3.75) and basic (pH = 9.3) conditions. The optimal LC separation of 16 different NAD⁺ metabolites was achieved using the hybrid Scherzo SM-C18 (3 μ m 2.0 mm \times 150 mm) reversed phase column (Imtakt, Portland, USA) with simultaneous cation and anion exchange thus allowing for improved retention and selectivity of polar metabolites (Table 1, Figure 1b). The mobile phase was composed of A = 20 mM ammonium formate and 0.1% formic acid in H₂O, and B = 20 mM ammonium formate and 0.1% formic acid (90:10, v/v) in acetonitrile. The gradient elution started at 100% A (0–2 min), reaching 100% B (at 12 min), then 100% B was held for 3 min and decreased to 100% A in 1 min following for an isocratic step at the initial conditions (16 min–22 min) for column re-equilibration. The flow rate was 200 μ L/min, column temperature 30°C, and the sample injection volume 2 μ L. To avoid the potential sample carryover, in both analytical conditions, the injection path was cleaned after each injection using a strong (0.2% formic acid in methanol) and weak solvent (0.2% formic acid in water).

Using the described method, the metabolite pairs with 1 Da difference, NA-Nicotinamide, NMN/NaMN, NR/NaR, and NAD/NADH/NaAD, in addition to several intermediates in the tryptophan-kynurenine pathway (a starting point of de novo NAD⁺ synthesis) were efficiently separated along the chromatographic gradient. The exception were the kynurenic (KA), picolinic (PA), and quinolinic acid (QA) for which the level of quantification was 17, 200, and 400 nM, respectively. Therefore, a complementary RPLC-MS/MS method (based on previously described conditions (Whiley et al., 2019)) was used to quantify these specific metabolites (method details are provided in Supplementary Information, Tables S2 and S4) with enhanced sensitivity.

The AJS ESI source conditions operating in positive mode were set as follows: dry gas temperature 290°C, nebulizer 45 psi and flow 12 L/min, sheath gas temperature 350°C and flow 12L/min, nozzle voltage +500V, and capillary voltage +4000V. Dynamic Multiple Reaction Monitoring (DMRM) acquisition mode with a total cycle of 600 ms was used operating at the optimal collision energy for each metabolite transition (Table 1 and Table S4).

2.5 | Targeted method performance

For all analytes, calibration curves were linear or fitted by linear regression with weighting, and coefficients of determination (r^2) were greater than 0.98 except for anthranilic acid ($r^2 = 0.946$) and quinolinic acid ($r^2 = 0.929$, power fitted) (Table S2). Method precision was evaluated by determining intra- and inter-day measurement reproducibility in independently prepared pool of human plasma and brain tissue lysates (nine replicates analyzed per matrix, per day and over three different days, Table S5). The evaluated analytical reproducibility comprised the variability of sample preparation and of the LC-MS/MS analysis, and was matrix dependent. For the metabolites measured in the brain tissue matrix, the coefficient of variation (CV) was between 2% and 20%

**TABLE 1** List of NAD⁺metabolites (with their corresponding internal standards - IS) that were quantified using reversed phase LC column with weak ionic exchange (Scherzo SM-C18 column, Imtakt, Portland, USA)

| Metabolite | Pathway | Precursor [M + H] ⁺ | Quantifier product ion (CE) | Qualifier product ion (CE) | Retention time (min) | Internal standard (IS) |
|---|--------------------------------|--------------------------------|-----------------------------|----------------------------|----------------------|------------------------|
| Tryptophan (Trp) | De novo synthesis | 205.1 | 188.0 (8 eV) | 146.0 (20 eV) | 6.8 | Trp - 15N2 |
| Kynurenine (Kyn) | De novo synthesis | 209.1 | 192.0 (8 eV) | 146.0 (20 eV) | 6.2 | Kyn-d6 |
| Kynurenic acid (KA) | De novo synthesis | 190.1 | 116.0 (36 eV) | 144.0 (20 eV) | 9.5 | KA-d5 |
| Anthranilic acid (AA) | De novo synthesis | 138.1 | 120.0 (12 eV) | - | 9 | AA - 13C6 |
| 3-OH-Kynurenine (3-OH-Kyn) | De novo synthesis | 225.1 | 162.0 (20 eV) | 110.0 (10 eV) | 5.6 | 3-OH-Kyn -13C3;15N |
| Xanthurenic acid (XA) | De novo synthesis | 206.0 | 160.0 (20 eV) | 132.0 (32 eV) | 9.3 | |
| 3-OH-Anthranilic acid (3-OH-AA) | De novo synthesis | 154.1 | 136.0 (10 eV) | 108.0 (20 eV) | 7.5 | |
| Picolinic acid (PA) | De novo synthesis | 124.0 | 51.0 (40 eV) | 106.0 (5 eV) | 3.5 | PA-d3 |
| Quinolinic acid (QA) | De novo synthesis | 168.0 | 78.0 (20 eV) | 150.0 (5 eV) | 7.5 | QA - 13C3;15N |
| Nicotinic acid mononucleotide (NaMN) | De novo synthesis [#] | 336.1 | 124.0 (12 eV) | 96.9 (20 eV) | 3.6 | NaMN-d4 |
| Nicotinic acid adenine dinucleotide (NaAD) | De novo synthesis [#] | 665.1 | 524.1 (16 eV) | 136.1 (40 eV) | 7.4 | |
| Nicotinamide adenine dinucleotide (NAD ⁺) | De novo synthesis [#] | 664.1 | 136.0 (40 eV) | 428.0 (24 eV) | 5.7 | NAD - 13C5 |
| Nicotinamide (NAM) | Salvage | 123.1 | 80.0 (24 eV) | 78.0 (36 eV) | 5.8 | NAM-d4 |
| Nicotinamide mononucleotide (NMN) | Salvage | 335.1 | 123.1 (12 eV) | 96.9 (28 eV) | 2.5 | |
| Nicotinamide Riboside (NR) | Salvage | 255.1 | 123.1 (24 eV) | 57.1 (16 eV) | 2.4 | |
| Nicotinic acid (NA) | Preiss-Handler | 124.0 | 78.0 (20 eV) | 80.5 (20 eV) | 4.0 | NA-d4 |
| Nicotinate Riboside (NaR) | Preiss-Handler | 256.1 | 124.1(32 eV) | 133.0 (8 eV) | 3.9 | |
| Nicotinamide adenine dinucleotide (NADH) | Preiss-Handler | 666.1 | 648.9 (20 eV) | 514.1 (28 eV) | 10. | |

To target and quantify these metabolites, the multiple reaction monitoring (MRM) parameters, including the quantifier and qualifier product ions, are provided together with respective collision energies (CEs) and retention times (RTs). Because of low sensitivity for the detection of quinolinic and picolinic acid, and a significant carryover of xanthurenic acid, the alternative method was optimized for these metabolites (including other intermediates in Trp - Kyn pathway (Table S5) with the exception of NMN / NaMN and NR / NaR metabolite pairs for which no separation was achieved with this complementary method). [#]NaMN, NaAD, and NAD⁺ are the intermediates of both de novo synthesis and Preiss-Handler pathway.

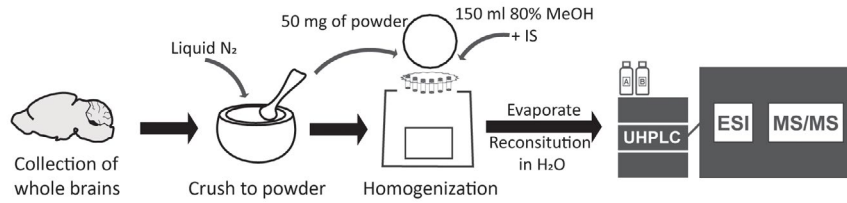
for intra- and inter-day measurements, with the exception of the NaR (CV = 25% for intra- and 38% for inter-day precision), which was detected at the concentration levels close to the limit of quantification (Table S5). For human plasma analysis, the measurement precision was also between 2% and 20% for all the intermediates with the exception of NMN (CV = 24% for intra- and 41% for inter-day precision).

2.6 | Experimental design and animal harvesting

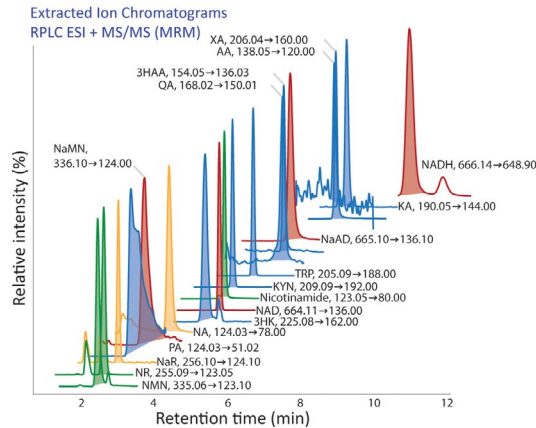
All experimental procedures were approved by the Veterinary Affairs Office of the Canton of Vaud, Switzerland (authorization number VD3106.c) and were conducted in strict accordance with the animal care guidelines outlined in the Swiss Ordinance on Animal

Experimentation to minimize the number and suffering of animals used in all experiments of this study. Animals were sacrificed by decapitation without anesthesia beforehand in accordance with the above specified legislation. The whole brain was snap-frozen immediately to minimize the potential ischemia that could affect labile metabolites (Dienel, 2021). Whenever possible and specifically when brain dissection is performed, the Focused Beam Microwave Irradiation (FBMI) should be applied for instantaneous euthanasia and halting of enzymatic activity (Epstein et al., 2013). However, the effect of required anesthesia (according to animal care guidelines) prior to FBMI remains poorly understood (Ivanisevic et al., 2014). Animals were sacrificed in three different batches over three different days (at 2 p.m.), each time in an arbitrary fashion with respect to animal genotype and sex. Overall, 32 specimens of 3xTg AD

(a) Sample preparation & analysis



(b) Metabolite separation and MS detection



(c) Data processing & analysis

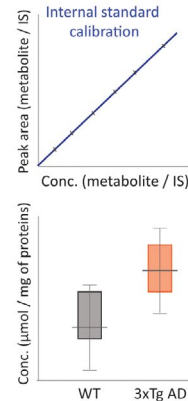


FIGURE 1 NAD⁺metabolite analysis pipeline, from (a) sample preparation to (b) LC-MS/MS analysis, including metabolite separation and targeted mass spectrometry-assisted quantification and (c) data processing and analysis. For metabolite extraction, brain tissue was homogenized with the addition of internal standards (IS spike) in methanol:water (4:1, v/v) using tissue homogenizer with cold trap (Precellys Cryolys). The NAD⁺metabolites present in the pre-concentrated tissue extract were injected into the LC-MS/MS system for separation (using reversed phase column with weak ionic ligands - Scherzo SM-C18, Imtakt, USA) and MS/MS detection in multiple reaction monitoring (MRM) mode using specific precursor → product ion transitions. Presented ion chromatograms were extracted from the standard mixture analysis. Concentration was determined based on the IS response and the calibration curve. Statistical analysis was performed following the data quality assessment. NAD⁺ de novo synthesis – blue peaks: TRP tryptophan, KYN kynurenine, KA kynurenic acid, 3HK 3-hydroxy-kynurenine, AA anthranilic acid, 3HAA 3-hydroxyanthranilic acid, XA xanthurenic acid, PA picolinic acid, QA quinolinic acid; 'NAD⁺ backbone' – red peaks: NaMN nicotinic acid mononucleotide, NaAD nicotinic acid adenine dinucleotide, NAD⁺ nicotinamide adenine dinucleotide and NADH nicotinamide adenine dinucleotide + hydrogen; Preiss-Handler pathway – yellow peaks: NaR nicotinic acid riboside, NA nicotinic acid; Salvage pathway – green peaks: NR nicotinamide riboside, nicotinamide, NMN nicotinamide mononucleotide

mouse (RRID:MMRRC_034830-JAX) and WT mouse (RRID:IMSR_JAX:101,045) were sacrificed in an arbitrary order, at the age of 29–32 weeks (depending on specimen), to reach 6–8 mice per group (see Figure 2). All specimens belonging to one same group presented the same genotype (WT or 3xTg AD) and were grown in the same controlled conditions; therefore, the number of biological replicates required was estimated to six (minimum) to capture the interindividual variability inherent to metabolome (Blaise et al., 2016). No randomization was performed to allocate subjects in the study and no

blinding, no sample size calculation, and no exclusion criteria were applied in the context of this exploratory study. The pre-registration of this study was not necessary according to the Swiss legislation.

2.7 | Brain tissue collection and homogenization

Whole brain was collected and immediately frozen on dry ice after decapitation of 3xTg AD and C7BL/6 mice. Mice metadata,

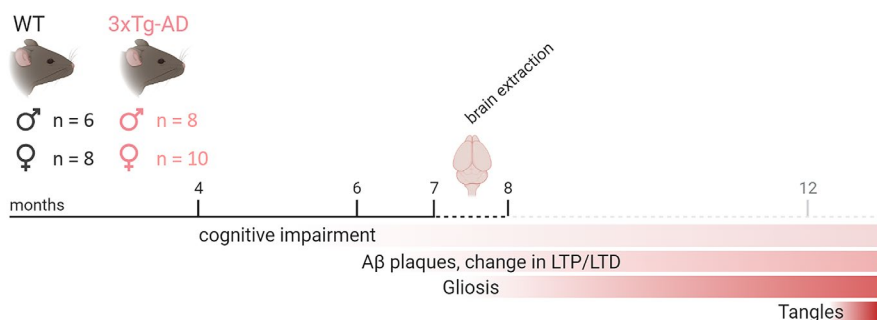


FIGURE 2 Sex-stratified design of the NAD⁺metabolism study in 3xTg AD mice versus WT at 8 months. LTP, long-term potentiation; LTD, long-term depression; WT, wild-type C7BL/6 mice; 3xTg AD mice, triple transgenic Alzheimer's disease mice



including the specimen's genotype, sex, tissue weight and total protein content are provided in the Table S3. Prior to metabolite extraction, brain tissue samples were mechanically homogenized under liquid nitrogen (using mortar and pestle), pre-weighed (~50 mg) in the lysis tubes (soft tissue CK 14 tubes, Bertin Technologies, Rockville, MD, US), and pre-extracted by the addition of ice-cold MeOH:H₂O (4:1; v:v) with 0.1% formic acid (150 μ L of solvent/10 mg of tissue) and ceramic beads, in the Cryolys Precellys 24 sample Homogenizer (2 \times 20 s at 10,000 rpm, Bertin Technologies). The bead beater was air-cooled with a flow rate at 110 L/min at 6 bar. Homogenized extracts were centrifuged for 15 min at 21'000 g at 4°C. The supernatant (metabolite extract) was removed and used as described below in the sample preparation section. Total protein content of the extracted tissue samples was determined for sample amount normalization. Protein pellets were resuspended in the in-house prepared lysis buffer (containing 20 mM Tris-HCl (pH 7.5), 150 mM NaCl, 1 mM Na₂EDTA, 1 mM EGTA, 1% Triton, 2.5 mM sodium pyrophosphate, 1 mM beta-glycerophosphate, 1 mM Na₃VO₄, and 1 μ g/ml leupeptin (Cell Lysis buffer, cat. no. 9,803, Cell Signaling Technology)) and 4 M guanidine hydrochloride (cat. no. G4505, Merck) using the Cryolys Precellys 24 sample Homogenizer (2 \times 20 s at 10,000 rpm). The BCA Protein Assay Kit (cat. no. 23,227, Thermo Scientific) was used to measure total protein concentration on a microplate reader at 562 nm (Hidex, Turku, Finland).

2.8 | Data processing

Data processing was performed using MassHunter Quantitative Analysis (for QqQ, version B.07.01/ Build 7.1.524.0, Agilent Technologies). Peak area integration was manually curated and concentrations were reported by selecting a 6-point portion of the linear standard curves relevant for the observed concentration range. Concentration of each compound was calculated as the peak area ratio between analyte and its corresponding internal standard. For the analytes without matching IS, quantification was performed using the external calibration method.

2.9 | Statistical data analysis

Group comparison was performed with the absolute concentration data, using a parametric two-way ANOVA to test for the effect of disease, sex, and their interaction on differences in metabolite concentrations (the assumptions of data normality and homogeneity of variance were tested beforehand using Shapiro-Wilk test and Levene's test, respectively). No tests for outliers were performed in this exploratory study. A *p*-value significance cut-off 0.05 (FDR <0.20) was used. The analyses were performed using R <https://www.r-project.org/>.

3 | RESULTS

3.1 | Altered NAD⁺ metabolism in 3xTg AD mice brain quantified using LC-MS/MS: Focus on sex differences

To gain insight into the potential alterations of NAD⁺ metabolism in the AD brain and evaluate the previously implied sex differences in AD manifestation, we performed the targeted metabolic phenotyping of 3xTg AD mice brain (*n* = 18) in a sex-balanced design, using C57BL/6 WT mice as a control (*n* = 14). Triple transgenic AD mouse presented specific features of AD pathology (A β plaques and gliosis) including the potential cognitive deficits (Figure 2) (Chiquita et al., 2019; Desai et al., 2009; Giménez-Llort et al., 2007). Using the developed targeted LC-MS/MS methods (see Materials and Methods for detailed description), the concentrations of nicotinate and nicotinamide intermediates in brain samples of 8-month-old AD and WT mice were successfully measured, including the Preiss-Handler and NAD⁺ salvage pathway and the tryptophan-kynurenine metabolites leading to de novo NAD⁺ synthesis.

3.2 | Preiss-Handler and NAD⁺ salvage pathway

In the mice brain lysates, eight NAD⁺ metabolites were quantified, including nicotinic acid (NA) and its dietary precursor NaR in the Preiss-Handler pathway and NaAD further downstream. Nicotinamide and NMN were quantified from the NAD⁺ salvage pathway, as well as NR, the dietary precursor of this pathway (Figure 3).

Within these pathways, significantly higher concentrations of NA were observed in AD mice compared to WT mice, both in males and in females ($P_{\text{genotype}} = 0.043$). Oppositely, in the NAD⁺ salvage pathway, significantly lower concentrations of NMN were observed in AD mice brain compared to WT mice brain, in both males and females ($P_{\text{genotype}} = 0.023$).

Importantly, significant sex differences in both genotypes were observed, with higher concentrations of NaAD ($P_{\text{sex}} = 0.016$) and NAD⁺ ($P_{\text{sex}} = 0.047$) and lower concentrations of nicotinamide ($P_{\text{sex}} = 0.012$) in males compared to females. Additionally, NaR concentrations ($P_{\text{sex}} = 0.029$) were higher in males than in females overall, but could be mainly attributed to significantly higher concentrations in male AD mice compared to its female counterparts ($P_{\text{interaction}} = 0.018$, Post-hoc $P_{\text{maleADvs.femaleAD}} = 0.011$). Similarly, significantly higher concentrations of NR were observed in male AD mice ($P_{\text{interaction}} = 0.00024$, Post-hoc $P_{\text{maleADvs.femaleAD}} = 0.0056$), for which the concentrations in female AD mice were also significantly lower than in the female WT mice ($p = .0022$).

3.3 | De novo NAD⁺ synthesis

Four metabolites of the de novo NAD⁺ synthesis pathway were detected and quantified in mice brain, that is, tryptophan (TRP) and kynurenine

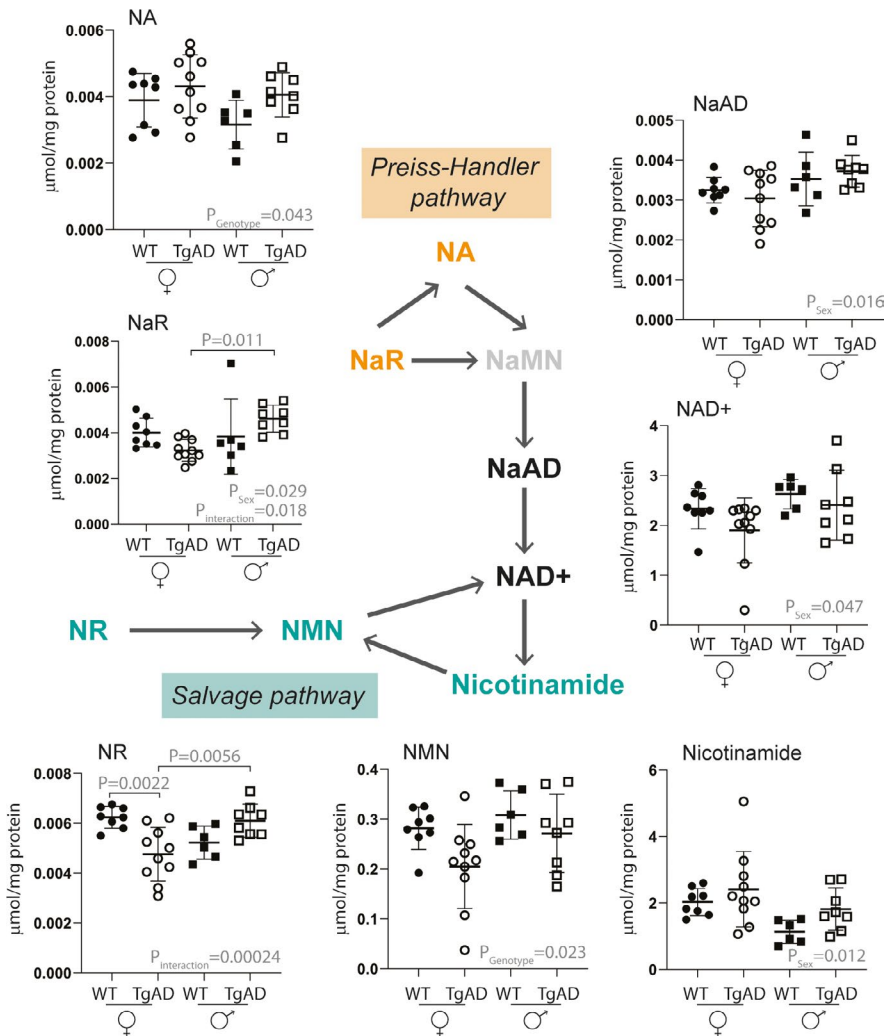


FIGURE 3 Levels of NAD⁺ metabolites in the Preiss-Handler and salvage pathway measured in brains of 8-month-old WT and 3xTg AD mice. All metabolites were quantified using RP chromatography with weak ionic exchange (Scherzo SM-C18, Table 1). Metabolite in gray was below the level of detection in AD and/or WT brain tissue. NA, nicotinic acid; NaR, nicotinic acid riboside; NaMN, nicotinic acid mononucleotide; NaAD, nicotinic acid adenine dinucleotide; NAD⁺, nicotinamide adenine dinucleotide; NR, nicotinamide riboside; NMN, nicotinamide mononucleotide. The P-values P_{Sex} , P_{Genotype} , and $P_{\text{Interaction}}$ result from ANOVA analysis using the following model: metabolite concentration = Sex * Genotype; p-values above graphs result from subsequent post-hoc analysis. Metabolite concentrations were reported to total protein content which was correlated with tissue weight and was not different between genotypes (Table S3).

(KYN) as well as kynurenic acid (KA) and xanthurenic acid (XA, Figure 4). KYN and KA concentrations were significantly different between the two genotypes with significantly higher concentrations in AD mice compared to WT mice. KYN concentrations were significantly lower in AD mice ($P_{\text{Genotype}} = 0.0014$), while KA concentrations were significantly higher in AD mice compared to WT mice ($P_{\text{Genotype}} = 0.0035$). For KA, this significant difference was mainly driven by males (i.e., attributable to significantly higher concentrations in male AD mice compared to male WT mice ($P_{\text{Interaction}} = 0.0083$, Post-hoc $P_{\text{maleADvs'maleWT}} = 0.0012$)). In addition, significantly higher KA concentrations were observed in male AD mice compared to female AD mice (Post-hoc $P_{\text{maleADvs'femaleAD}} = 0.040$). For kynurenine, the significant decrease was mainly driven by females ($P_{\text{femaleADvs'femaleWT}} = 0.02$). Finally, for tryptophan, no difference was observed with respect to genotype, but the significant sex difference was measured with higher concentration in female mice compared to male mice, in both AD and WT genotypes ($P_{\text{Sex}} = 0.0087$).

4 | DISCUSSION

The potential sex-specific alterations in NAD⁺ metabolism associated with AD pathology were investigated directly in the brain tissue

of 3xTg AD mouse model compared to WT, in a sex-balanced design (Figure 2). In mice brains, we successfully quantified 12 intermediates from all three routes of NAD⁺ production and demonstrated that the developed method was sensitive and accurate enough to capture metabolite level differences between WT and transgenic AD mouse brains, as well as between males and females. The chromatographic resolution allowed for the distinction between the challenging metabolite pairs (with 1 Da mass difference), comprising nicotinamide and NA, their riboside sources (NR / NaR), and mononucleotide products (NMN / NaMN)—direct precursors of NaAD and NAD⁺. These metabolites are highly relevant for their role in boosting the NAD⁺ production and are currently actively explored in numerous supplementation studies, for their beneficial effect in human nutrition and most importantly the preservation of healthy organ function with aging (Bulluck & Hausenloy, 2018; Giroud-Gerbetant et al., 2019; Hou et al., 2018; Katsyuba et al., 2018; Martens et al., 2018).

In de novo NAD⁺ synthesis, we have observed a significant AD-related decrease in kynurenine (34% lower than in WT) in both sexes and a significant AD-related increase in the levels of kynurenic acid, specifically in males (43% higher than in WT). This result suggests that a considerable portion of kynurenine might be

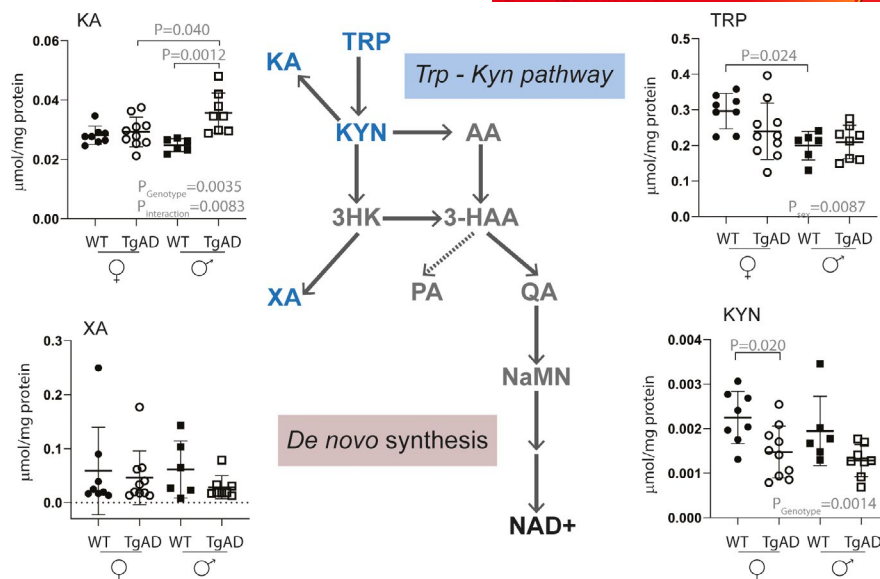


FIGURE 4 Levels of NAD⁺ metabolites in de novo synthesis measured in brains of 8-month-old WT and 3xTg AD mice. Tryptophan (TRP) and kynurenine (KYN) were quantified using RP chromatography with weak ionic exchange (Scherzo SM-C18 column, Table 1). Kynurenic acid (KA) and xanthurenic acid (XA) were quantified using standard RP chromatography (C18 HSS T3 column, Table S5); metabolites in gray were below the level of detection in AD and/or WT brain tissue. TRP tryptophan, KYN kynurenine, KA kynurenic acid, AA anthranilic acid, 3HK 3-hydroxy-kynurenine, 3HAA 3-hydroxyanthranilic acid, XA xanthurenic acid, PA picolinic acid, QA quinolinic acid, NaMN nicotinic acid mononucleotide, NaAD nicotinic acid adenine dinucleotide, NAD⁺ nicotinamide adenine dinucleotide. The p -values P_{Sex} , P_{genotype} , and $P_{\text{interaction}}$ result from ANOVA analysis metabolite concentration = Sex * Genotype; p -values above graphs result from subsequent post-hoc analysis. Metabolite concentrations were reported to total protein content which was correlated with tissue weight and was not different between genotypes (Table S3).

consumed for the production of neuroprotective kynurenic acid, which has documented anti-inflammatory and immunosuppressive functions, as a compensatory response to the neuroinflammatory process known to be present in AD (Wirthgen et al., 2017). Our results also imply that this mechanism might be regulated in a sex-specific manner (i.e., higher kynurenic acid concentrations in males). The hypothesis about the effect of circulating sex steroid hormones on the immune-regulating kynurenine pathway was recently emitted. A significantly lower concentrations of kynurenic acid were reported in healthy females (compared to males) and are thought to be implicated in the pathogenesis of mood disorders (Meier et al., 2018). Next to the association of changes in the levels of kynurenine pathway metabolites with the neuroinflammation, several degradation products, including the anthranilic acid and quinolinic acid, are of interest for their potential immune- and neuromodulatory functions. In this context, an altered balance between the kynurenic and quinolinic acid was reported in CSF in several neurological disorders (Kindler et al., 2020; Savitz et al., 2015; Wirthgen et al., 2017). In our study, quinolinic acid as well as its precursors anthranilic and hydroxy-anthranilic acid were below the level of detection in the analyzed brain tissue, thus hindering further insights into this balance in 3xTg AD model.

Changes in the NAD⁺ de novo synthesis, that is, the tryptophan/kynurenine pathway, related to AD were previously reported in several human case-control studies comparing plasma and CSF concentrations in AD patients versus controls. The levels of several metabolites were found to be significantly increased or decreased

in AD (Giil et al., 2017; Sorgdrager et al., 2019; van der Velpen et al., 2019), of which some were associated with core AD pathology or AD severity (Jacobs et al., 2021; Sorgdrager et al., 2019; van der Velpen et al., 2019). However, it is important to highlight that some changes in this pathway, specifically related to kynurenic acid levels, were also attributed to age (de Bie et al., 2016; Giil et al., 2017).

Finally, our results showed a significant decrease in the concentrations of nicotinamide mononucleotide (NMN) in the brain of 3xTg AD mice model compared to the WT mice. The decrease of this precursor of NAD⁺ in the salvage pathway was more pronounced in females than in males (27% vs. 12% lower than in WT, respectively). The depletion of NMN levels (due to impaired conversion from nicotinamide and/or NR) might significantly impact the replenishment of NAD⁺ also because the salvage pathways (including the Preiss-Handler pathway) are assumed to be the main source of NAD⁺, requiring the uptake of its precursors from the diet (Houtkooper et al., 2010). In our study, significantly higher concentrations of NR and NaR were found in 3xTg males compared to females which might be because of the differences in the absorption and/or the consumption process, as well as the dietary intake. The discussion on the changes in these dietary metabolite concentrations (NR, NaR, and NA) is therefore challenging with respect to the lack of data on mice dietary regimen and habits. However, tracking the fate of these metabolites would be of utmost importance in the future supplementation studies.

Overall, we have observed a tendency of decline in NAD⁺ levels in 3xTg AD mouse model, which was not statistically significant. This

might be related to the disease stage at the time of brain collection that preceded the accumulation of Tau tangles and neuronal death (Hou et al., 2018), although other behavioral and neuronal symptoms of AD were previously reported to be present in 8-month-old 3xTg mouse model (Desai et al., 2009; Giménez-Llort et al., 2007). The compensatory mechanisms might still be functional at this stage of AD progression to prevent the loss of metabolic homeostasis, which leads to irreversible changes in energy metabolism (Ivanisevic et al., 2016).

Our results suggest that several routes of NAD⁺ replenishment (including de novo synthesis and salvage pathway(s)) appear to be affected in the AD brain and that, therefore, the NAD⁺ decline might not be mainly related to the increased consumption of NAD⁺ by sirtuins, PARP, and CD38 (in the control of signaling and transcriptional events). This widens the opportunities for interventions to maintain the NAD⁺ levels (through supplementation or gene modulation), vital to preserve the functioning of mitochondria, ATP production, and neuronal function. Many hypothesize that efficient maintenance of NAD⁺ levels could prevent the decreased function of neurons and their death with age as well as the progression of AD. Supplementation of the NAD⁺ precursors nicotinamide (NAM), nicotinamide riboside (NR), and nicotinamide mononucleotide (NMN) have shown to boost the NAD⁺ levels in several mouse models, mainly through the regulation of its downstream degradation (SIRT and PARP). The decreased amyloid and tau burden in AD mouse models and related cell cultures were also reported (Lautrup et al., 2019). In humans, clinical trials to date have found that circulating NAD⁺ levels can indeed be increased, although effects on improved cognitive performance in AD and MCI remain inconsistent (Lautrup et al., 2019). Finally, our results confirm that the sex represents an important factor in AD pathology (Carroll et al., 2007; Clinton et al., 2007), thus warranting the careful use of male and female specimens in animal model studies and the consideration of sex effects in human studies.

ACKNOWLEDGMENTS

The authors thank the Foundation Pierre Mercier pour la science for the financial support of Vera van der Velpen (research grant to JI), the Synapsis Foundation - Alzheimer Research Switzerland ARS (research grant to JYC), and the Faculty of Biology and Medicine, University of Lausanne for regular annual funding.

All experiments were conducted in compliance with the ARRIVE guidelines.

CONFLICT OF INTEREST

The authors declare no competing financial interest.

ORCID

Jean-Yves Chatton  <https://orcid.org/0000-0002-8911-0315>

Julijana Ivanisevic  <https://orcid.org/0000-0001-8267-2705>

REFERENCES

Arnold, M., Nho, K., Kueider-Paisley, A., Massaro, T., Huynh, K., Brauner, B., MahmoudianDehkordi, S., Louie, G., Moseley, M. A., Thompson,

J. W., St John-Williams, L., Tenenbaum, J. D., Blach, C., Chang, R., Brinton, R. D., Baillie, R., Han, X., Trojanowski, J. Q., Shaw, L. M., ... Kastenmüller, G. (2020). Sex and APOE epsilon4 genotype modify the Alzheimer's disease serum metabolome. *Nature Communications*, *11*, 1148.

Association, A. S. (2020). 2020 Alzheimer's disease facts and figures. *Alzheimer's & Dementia: the Journal of the Alzheimer's Association*, *16*, 391.

Blaise, B. J., Correia, G., Tin, A., Young, J. H., Vergnaud, A.-C., Lewis, M., Pearce, J. T. M., Elliott, P., Nicholson, J. K., Holmes, E., & Ebbs, T. M. D. (2016). Power analysis and sample size determination in metabolic phenotyping. *Analytical Chemistry*, *88*, 5179–5188.

Bulluck, H., & Hausenloy, D. J. (2018). Modulating NAD⁺ metabolism to prevent acute kidney injury. *Nature Medicine*, *24*, 1306–1307.

Bustamante, S., Jayasena, T., Richani, D., Gilchrist, R. B., Wu, L. E., Sinclair, D. A., Sachdev, P. S., & Braidy, N. (2017). Quantifying the cellular NAD⁺ metabolome using a tandem liquid chromatography mass spectrometry approach. *Metabolomics*, *14*, 15. <https://doi.org/10.1007/s11306-017-1310-z>

Canto, C., Menzies, K. J., & Auwerx, J. (2015). NAD(+) Metabolism and the control of energy homeostasis: A balancing act between mitochondria and the nucleus. *Cell Metabolism*, *22*, 31–53. <https://doi.org/10.1016/j.cmet.2015.05.023>

Carroll, J. C., Rosario, E. R., Chang, L., Stanczyk, F. Z., Oddo, S., LaFerla, F. M., & Pike, C. J. (2007). Progesterone and estrogen regulate Alzheimer-like neuropathology in female 3xTg-AD mice. *The Journal of Neuroscience: The Official Journal of the Society for Neuroscience*, *27*, 13357–13365. <https://doi.org/10.1523/JNEUROSCI.2718-07.2007>

Chiquita, S., Ribeiro, M., Castelhan, J., Oliveira, F., Sereno, J., Batista, M., Abrunhosa, A., Rodrigues-Neves, A. C., Carecho, R., Baptista, F., Gomes, C., Moreira, P. I., Ambrósio, A. F., & Castelo-Branco, M. (2019). A longitudinal multimodal in vivo molecular imaging study of the 3xTg-AD mouse model shows progressive early hippocampal and taurine loss. *Human Molecular Genetics*, *28*, 2174–2188. <https://doi.org/10.1093/hmg/ddz045>

Clement, J., Wong, M., Poljak, A., Sachdev, P., & Braidy, N. (2019). The plasma NAD(+) metabolome is dysregulated in "Normal" aging. *Rejuvenation Research*, *22*, 121–130.

Clinton, L. K., Billings, L. M., Green, K. N., Caccamo, A., Ngo, J., Oddo, S., McGaugh, J. L., & LaFerla, F. M. (2007). Age-dependent sexual dimorphism in cognition and stress response in the 3xTg-AD mice. *Neurobiology of Disease*, *28*, 76–82. <https://doi.org/10.1016/j.nbd.2007.06.013>

Darst, B. F., Kosciak, R. L., Hogan, K. J., Johnson, S. C., & Engelman, C. D. (2019). Longitudinal plasma metabolomics of aging and sex. *Aging (Albany NY)*, *11*, 1262–1282. <https://doi.org/10.18632/aging.101837>

de Bie, J., Guest, J., Guillemin, G. J., & Grant, R. (2016). Central kynurenine pathway shift with age in women. *Journal of Neurochemistry*, *136*, 995–1003. <https://doi.org/10.1111/jnc.13496>

Desai, M. K., Sudol, K. L., Janelins, M. C., Mastrangelo, M. A., Frazer, M. E., & Bowers, W. J. (2009). Triple-transgenic Alzheimer's disease mice exhibit region-specific abnormalities in brain myelination patterns prior to appearance of amyloid and tau pathology. *Glia*, *57*, 54–65. <https://doi.org/10.1002/glia.20734>

Dienel, G. A. (2021). Stop the rot. Enzyme inactivation at brain harvest prevents artifacts: A guide for preservation of the in vivo concentrations of brain constituents. *Journal of Neurochemistry*, 1–25. <https://doi.org/10.1111/jnc.15293>

Epstein, A. A., Narayanasamy, P., Dash, P. K., High, R., Bathena, S. P. R., Gorantla, S., Poluektova, L. Y., Alnouti, Y., Gendelman, H. E., & Boska, M. D. (2013). Combinatorial assessments of brain tissue metabolomics and histopathology in rodent models of human immunodeficiency virus infection. *Journal of Neuroimmune Pharmacology: the Official Journal of the Society on NeuroImmune Pharmacology*, *8*, 1224–1238. <https://doi.org/10.1007/s11481-013-9461-9>

- Ferretti, M. T., Iulita, M. F., Cavedo, E., Chiesa, P. A., Schumacher Dimech, A., Santuccione Chadha, A., Baracchi, F., Girouard, H., Misoch, S., Giacobini, E., Depypere, H., & Hampel, H. (2018). Sex differences in Alzheimer disease — the gateway to precision medicine. *Nature Reviews Neurology*, *14*, 457–469. <https://doi.org/10.1038/s41582-018-0032-9>
- Gallart-Ayala, H., Teav, T., & Ivanisevic, J. (2020). Metabolomics meets lipidomics: Assessing the small molecule component of metabolism. *BioEssays*, *42*, e2000052.
- Giil, L. M., Middttun, Ø., Refsum, H., Ulvik, A., Advani, R., Smith, A. D., & Ueland, P. M. (2017). Kynurenine pathway metabolites in Alzheimer's disease. *Journal of Alzheimer's Disease*, *60*, 495–504. <https://doi.org/10.3233/JAD-170485>
- Giménez-Llort, L., Blázquez, G., Cañete, T., Johansson, B., Oddo, S., Tobeña, A., LaFerla, F. M., & Fernández-Teruel, A. (2007). Modeling behavioral and neuronal symptoms of Alzheimer's disease in mice: A role for intraneuronal amyloid. *Neuroscience and Biobehavioral Reviews*, *31*, 125–147. <https://doi.org/10.1016/j.neubiorev.2006.07.007>
- Giroud-Gerbetant, J., Joffraud, M., Giner, M. P., Cercillieux, A., Bartova, S., Makarov, M. V., Zapata-Pérez, R., Sánchez-García, J. L., Houtkooper, R. H., Migaud, M. E., Moco, S., & Canto, C. (2019). A reduced form of nicotinamide riboside defines a new path for NAD⁺ biosynthesis and acts as an orally bioavailable NAD⁺ precursor. *Molecular Metabolism*, *30*, 192–202. <https://doi.org/10.1016/j.molmet.2019.09.013>
- Hikosaka, K., Yaku, K., Okabe, K., & Nakagawa, T. (2021). Implications of NAD metabolism in pathophysiology and therapeutics for neurodegenerative diseases. *Nutritional Neuroscience*, *24*(5), 371–383. <https://doi.org/10.1080/1028415X.2019.1637504>
- Hou, Y., Lautrup, S., Cordonnier, S. et al (2018). NAD(+) supplementation normalizes key Alzheimer's features and DNA damage responses in a new AD mouse model with introduced DNA repair deficiency. *Proceedings of the National Academy of Sciences of the United States of America*, *115*, E1876–e1885.
- Houtkooper, R. H., Canto, C., Wanders, R. J., & Auwerx, J. (2010). The secret life of NAD⁺: An old metabolite controlling new metabolic signaling pathways. *Endocrine Reviews*, *31*, 194–223. <https://doi.org/10.1210/er.2009-0026>
- Houtkooper, R. H., Cantó, C., Wanders, R. J., & Auwerx, J. (2010). The secret life of NAD⁺: An old metabolite controlling new metabolic signaling pathways. *Endocrine Reviews*, *31*, 194–223. <https://doi.org/10.1210/er.2009-0026>
- Imai, S., & Guarente, L. (2014). NAD⁺ and sirtuins in aging and disease. *Trends in Cell Biology*, *24*, 464–471. <https://doi.org/10.1016/j.tcb.2014.04.002>
- Ivanisevic, J., Epstein, A. A., Kurczy, M. E., Benton, P. H., Uritboonthai, W., Fox, H. S., Boska, M. D., Gendelman, H. E., & Siuzdak, G. (2014). Brain region mapping using global metabolomics. *Chemistry & Biology*, *21*, 1575–1584.
- Ivanisevic, J., Stauch, K. L., Petrascheck, M., Benton, H. P., Epstein, A. A., Fang, M., Gorantla, S., Tran, M., Hoang, L., Kurczy, M. E., Boska, M. D., Gendelman, H. E., Fox, H. S., & Siuzdak, G. (2016). Metabolic drift in the aging brain. *Aging*, *8*, 1000–1020. <https://doi.org/10.18632/aging.100961>
- Jacobs, H. I. L., Riphagen, J. M., Ramakers, I. H. G. B., & Verhey, F. R. J. (2021). Alzheimer's disease pathology: Pathways between central norepinephrine activity, memory, and neuropsychiatric symptoms. *Molecular Psychiatry*, *26*, 897–906.
- Katsyuba, E., & Auwerx, J. (2017). Modulating NAD(+) metabolism, from bench to bedside. *EMBO Journal*, *36*, 2670–2683.
- Katsyuba, E., Mottis, A., Zietak, M., De Franco, F., van der Velpen, V., Gariani, K., Ryu, D., Cialabrini, L., Matilainen, O., Liscio, P., Giacchè, N., Stokar-Regenscheit, N., Legouis, D., de Seigneux, S., Ivanisevic, J., Raffaelli, N., Schoonjans, K., Pellicciari, R., & Auwerx, J. (2018). De novo NAD(+) synthesis enhances mitochondrial function and improves health. *Nature*, *563*, 354–359. <https://doi.org/10.1038/s41586-018-0645-6>
- Kindler, J., Lim, C. K., Weickert, C. S., Boerigter, D., Galletly, C., Liu, D., Jacobs, K. R., Balzan, R., Bruggemann, J., O'Donnell, M., Lenroot, R., Guillemin, G. J., & Weickert, T. W. (2020). Dysregulation of kynurenine metabolism is related to proinflammatory cytokines, attention, and prefrontal cortex volume in schizophrenia. *Molecular Psychiatry*, *25*, 2860–2872. <https://doi.org/10.1038/s41380-019-0401-9>
- Lautrup, S., Sinclair, D. A., Mattson, M. P., & Fang, E. F. (2019). NAD⁺ in brain aging and neurodegenerative disorders. *Cell Metabolism*, *30*, 630–655. <https://doi.org/10.1016/j.cmet.2019.09.001>
- Lu, W., Bennett, B. D., & Rabinowitz, J. D. (2008). Analytical strategies for LC-MS-based targeted metabolomics. *Journal of chromatography. B, Analytical Technologies in the Biomedical and Life Sciences*, *871*, 236–242. <https://doi.org/10.1016/j.jchromb.2008.04.031>
- Martens, C. R., Denman, B. A., Mazzo, M. R., Armstrong, M. L., Reisdorph, N., McQueen, M. B., Chonchol, M., & Seals, D. R. (2018). Chronic nicotinamide riboside supplementation is well-tolerated and elevates NAD(+) in healthy middle-aged and older adults. *Nature Communications*, *9*, 1286.
- Martino Carpi, F., Cortese, M., Orsomando, G., Polzonetti, V., Vincenzetti, S., Moreschini, B., Coleman, M., Magni, G., & Pucciarelli, S. (2018). Simultaneous quantification of nicotinamide mononucleotide and related pyridine compounds in mouse tissues by UHPLC-MS/MS. *Separation Science plus*, *1*, 22–30. <https://doi.org/10.1002/sscp.201700024>
- Massudi, H., Grant, R., Braid, N., Guest, J., Farnsworth, B., & Guillemin, G. J. (2012). Age-associated changes in oxidative stress and NAD⁺ metabolism in human tissue. *PLoS One*, *7*, e42357. <https://doi.org/10.1371/journal.pone.0042357>
- Meier, T. B., Drevets, W. C., Teague, T. K., Wurfel, B. E., Mueller, S. C., Bodurka, J., Dantzer, R., & Savitz, J. (2018). Kynurenic acid is reduced in females and oral contraceptive users: Implications for depression. *Brain, Behavior, and Immunity*, *67*, 59–64. <https://doi.org/10.1016/j.bbi.2017.08.024>
- Mielke, M. M. (2018). Sex and gender differences in Alzheimer's disease dementia. *Psychiatric Times*, *35*, 14–17.
- Mitchell, S. J., Bernier, M., Aon, M. A., Cortassa, S., Kim, E. Y., Fang, E. F., Palacios, H. H., Ali, A., Navas-Enamorado, I., Di Francesco, A., Kaiser, T. A., Waltz, T. B., Zhang, N., Ellis, J. L., Elliott, P. J., Frederick, D. W., Bohr, V. A., Schmidt, M. S., Brenner, C., ... de Cabo, R. (2018). Nicotinamide improves aspects of healthspan, but not lifespan, in mice. *Cell Metabolism*, *27*, 667–676.e664. <https://doi.org/10.1016/j.cmet.2018.02.001>
- Mouchiroud, L., Houtkooper, R. H., & Auwerx, J. (2013). NAD⁺ metabolism: A therapeutic target for age-related metabolic disease. *Critical Reviews in Biochemistry and Molecular Biology*, *48*, 397–408.
- Oddo, S., Caccamo, A., Shepherd, J. D., Murphy, M. P., Golde, T. E., Kayed, R., Metherate, R., Mattson, M. P., Akbari, Y., & LaFerla, F. M. (2003). Triple-transgenic model of Alzheimer's disease with plaques and tangles: Intracellular Aβ and synaptic dysfunction. *Neuron*, *39*, 409–421. [https://doi.org/10.1016/S0896-6273\(03\)00434-3](https://doi.org/10.1016/S0896-6273(03)00434-3)
- Rajman, L., Chwalek, K., & Sinclair, D. A. (2018). Therapeutic potential of NAD-boosting molecules: The in vivo evidence. *Cell Metabolism*, *27*, 529–547.
- Ratajczak, J., Joffraud, M., Trammell, S. A. J., Ras, R., Canela, N., Boutant, M., Kulkarni, S. S., Rodrigues, M., Redpath, P., Migaud, M. E., Auwerx, J., Yanes, O., Brenner, C., & Cantó, C. (2016). NRK1 controls nicotinamide mononucleotide and nicotinamide riboside metabolism in mammalian cells. *Nature Communications*, *7*, 13103. <https://doi.org/10.1038/ncomms13103>
- Roberts, L. D., Souza, A. L., Gerszten, R. E., & Clish, C. B. (2012). Targeted metabolomics. *Current Protocols in Molecular Biology*, *98*(1), 30.2.1–30.2.24.

- Rubio, V. Y., Cagmat, J. G., Wang, G. P., Yost, R. A., & Garrett, T. J. (2020). Analysis of tryptophan metabolites in serum using wide-isolation strategies for UHPLC–HRMS/MS. *Analytical Chemistry*, *92*, 2550–2557. <https://doi.org/10.1021/acs.analchem.9b04210>
- Sadok, I., Rachwal, K., & Staniszevska, M. (2019). Application of the optimized and validated LC-MS method for simultaneous quantification of tryptophan metabolites in culture medium from cancer cells. *Journal of Pharmaceutical and Biomedical Analysis*, *176*, 112805. <https://doi.org/10.1016/j.jpba.2019.112805>
- Savitz, J., Dantzer, R., Wurfel, B. E., Victor, T. A., Ford, B. N., Bodurka, J., Bellgowan, P. S., Teague, T. K., & Drevets, W. C. (2015). Neuroprotective kynurenine metabolite indices are abnormally reduced and positively associated with hippocampal and amygdalar volume in bipolar disorder. *Psychoneuroendocrinology*, *52*, 200–211. <https://doi.org/10.1016/j.psyneuen.2014.11.015>
- Scheltens, P., Blennow, K., Breteler, M. M. B., de Strooper, B., Frisoni, G. B., Salloway, S., & Van der Flier, W. M. (2016). Alzheimer's disease. *The Lancet*, *388*, 505–517. [https://doi.org/10.1016/S0140-6736\(15\)01124-1](https://doi.org/10.1016/S0140-6736(15)01124-1)
- Shi, H., Enriquez, A., Rapadas, M., Martin, E. M. M. A., Wang, R., Moreau, J., Lim, C. K., Szot, J. O., Ip, E., Hughes, J. N., Sugimoto, K., Humphreys, D. T., McInerney-Leo, A. M., Leo, P. J., Maghazal, G. J., Halliday, J., Smith, J., Colley, A., Mark, P. R., ... Dunwoodie, S. L. (2017). NAD deficiency, congenital malformations, and niacin supplementation. *New England Journal of Medicine*, *377*, 544–552. <https://doi.org/10.1056/NEJMoa1616361>
- Sorgdrager, F. J. H., Vermeiren, Y., Van Faassen, M., van der Ley, C., Nollen, E. A. A., Kema, I. P., & De Deyn, P. P. (2019). Age- and disease-specific changes of the kynurenine pathway in Parkinson's and Alzheimer's disease. *Journal of Neurochemistry*, *151*, 656–668. <https://doi.org/10.1111/jnc.14843>
- van der Velpen, V., Teav, T., Gallart-Ayala, H., Mehl, F., Konz, I., Clark, C., Oikonomidi, A., Peyratout, G., Henry, H., Delorenzi, M., Ivanisevic, J., & Popp, J. (2019). Systemic and central nervous system metabolic alterations in Alzheimer's disease. *Alzheimer's Research & Therapy*, *11*, 93. <https://doi.org/10.1186/s13195-019-0551-7>
- Whiley, L., Nye, L. C., Grant, I., Andreas, N., Chappell, K. E., Sarafian, M. H., Misra, R., Plumb, R. S., Lewis, M. R., Nicholson, J. K., Holmes, E., Swann, J. R., & Wilson, I. D. (2019). Ultrahigh-performance liquid chromatography tandem mass spectrometry with electrospray ionization quantification of tryptophan metabolites and markers of gut health in serum and plasma-application to clinical and epidemiology cohorts. *Analytical Chemistry*, *91*, 5207–5216. <https://doi.org/10.1021/acs.analchem.8b05884>
- Wirthgen, E., Hoeflich, A., Rebl, A., & Günther, J. (2017). Kynurenine acid: The Janus-faced role of an immunomodulatory tryptophan metabolite and its link to pathological conditions. *Frontiers in Immunology*, *8*, 1957. <https://doi.org/10.3389/fimmu.2017.01957>
- Wishart, D. S., Feunang, Y. D., Marcu, A. et al (2018). HMDB 4.0: The human metabolome database for 2018. *Nucleic Acids Research*, *46*, D608–d617.
- Yaku, K., Okabe, K., & Nakagawa, T. (2018a). NAD metabolism: Implications in aging and longevity. *Ageing Research Reviews*, *47*, 1–17. <https://doi.org/10.1016/j.arr.2018.05.006>
- Yaku, K., Okabe, K., & Nakagawa, T. (2018b). Simultaneous measurement of NAD metabolome in aged mice tissue using liquid chromatography tandem-mass spectrometry. *Biomedical Chromatography*, *32*, e4205. <https://doi.org/10.1002/bmc.4205>
- Yu, E., Papandreou, C., Ruiz-Canela, M. et al (2018). Association of tryptophan metabolites with incident Type 2 diabetes in the PREDIMED trial: A case-cohort study. *Clinical Chemistry*, *64*, 1211–1220.
- Zhu, X. H., Lu, M., Lee, B. Y., Ugurbil, K., & Chen, W. (2015). In vivo NAD assay reveals the intracellular NAD contents and redox state in healthy human brain and their age dependences. *Proceedings of the National Academy of Sciences*, *112*, 2876–2881. <https://doi.org/10.1073/pnas.1417921112>

SUPPORTING INFORMATION

Additional Supporting Information may be found online in the Supporting Information section.

How to cite this article: van der Velpen V, Rosenberg N, Maillard V, et al. Sex-specific alterations in NAD⁺ metabolism in 3xTg Alzheimer's disease mouse brain assessed by quantitative targeted LC-MS. *J Neurochem*. 2021;159:378–388. <https://doi.org/10.1111/jnc.15362>